MATERIALLY EFFICIENT THERMOMECHANICAL STUDY PROCEDURE FOR ROCKS PRESENTED ON A GLAUCONITIC SANDSTONE

Marek Brabec[*,1], Daniela Marková[1], Juraj Štetiar[1], Vojtěch Boltnar[1]

[*]marek.brabec.mb@gmail.com
[1]Brno University of Technology, Faculty of Civil Engineering, Institute of Geotechnics, Veveří 331/95, 602 00 Brno, Czech Republic

Abstract

Proper thermomechanical study of a rock type is typically significantly more expensive than a standard mechanical study in terms of geomaterial consumption. Multiple specimen sets (each sufficient for a standalone mechanical study) have to be produced for various target temperatures to obtain a comprehensive thermomechanical profile of the rock type. A possible solution for lowering the number of required specimens using a type II "multiple failure state" triaxial test is tested in this paper.

Keywords

Rock thermomechanics, temperature influence, type II triaxial test, material efficiency, glauconitic sandstone

1 INTRODUCTION

The general strength of rock mass is defined by a failure criterion, which envelops all possible states of stress the rock can withstand before failure [1]. In geotechnics, two failure criteria are most commonly used for the description of rock strength – linear Mohr-Coulomb (MC) and nonlinear Hoek-Brown (HB). Both typically require the execution of multiple individual conventional triaxial tests (CTTs). The CTTs are usually supplemented by additional uniaxial compressive tests (UCTs), as they can be considered as a subtype of CTT with confining pressure equal to 0 MPa. The test results are subsequently plotted and fitted with the criterion-specific curves for the determination of the key criterion parameters. At least three compressive tests at different confining pressures should be conducted to accurately characterise the rock strength and minimize the effect of specimen variability. However, a total of at least nine tests (three at each confining pressure) is preferable for reliable estimation [2].

The thermomechanical study of a specific rock type introduces an additional challenge, as it requires characterising rock strength across the entire relevant temperature range. The range is typically divided into several subranges (i.e. temperature steps, e.g. [3]). The steps must be sufficiently short to accurately capture the real trend of the criterion temperature dependence. Each temperature step requires an individual set of specimens to be prepared and tested, potentially overcoming the amount of available geomaterial.

The objective of this paper is to determine a thermomechanical profile of a local glauconitic sandstone (marine psammitic sediment from Bohemian Massif) with limited access to material for specimen production. A type II "multiple failure state" triaxial test (CTT_{II}) described in [4] is implemented instead of the more widely performed type I "individual" triaxial test (CTT_{I}) to obtain enough data for calibration of multiple failure criteria. The main advantage of the CTT_{II} over CTT_{I} is the ability to describe the entire failure criterion using only one specimen at the cost of a more demanding realisation procedure (see Fig. 1a for typical stress paths of UCT, CTT_{I} and CTT_{II}).

2 METHODOLOGY

The first step involved preparing cylindrical specimens from pre-sampled sandstone cores stored in the Institute of Geotechnics collection. In total, cores of two diameters with five samples each were available (38.1 mm and 54.6 mm). As the core samples were relatively short, each yielded only one cylindrical specimen produced using a circular saw with a diamond cutting disc. The target length-to-diameter ratio was 2.0 to comply with the relevant standard [2]. The smaller cores were used for the preparation of specimens for the CTT_{II}s, and the larger cores for

Received 27/01/2025/Accepted 28/03/2025/Published 30/09/2025 DOI 10.13164/juniorstav.2025.25032

the additional UCTs, resulting in five specimen sets available. After preparation, all specimens were carefully measured using a digital calliper and weighed on a laboratory scale for bulk density determination. One specimen set was left in a natural state and the other four were prepared for firing. A temperature step of 200°C was chosen to achieve a reasonable profile resolution while describing a wide temperature range (target temperatures: 20, 200, 400, 600 and 800°C). The specimens were fired according to a simple firing curve – increasing temperature by 5°C/min until the target temperature was reached, then holding the target temperature for an hour, after which the specimens were air-cooled in the furnace (see Fig. 1b). After firing, all specimens were re-measured and weighed to monitor temperature-induced changes in specimen volume and bulk density. Additionally, the cut surfaces of the specimen bases were examined under a microscope to study visible alterations in the sandstone matrix.

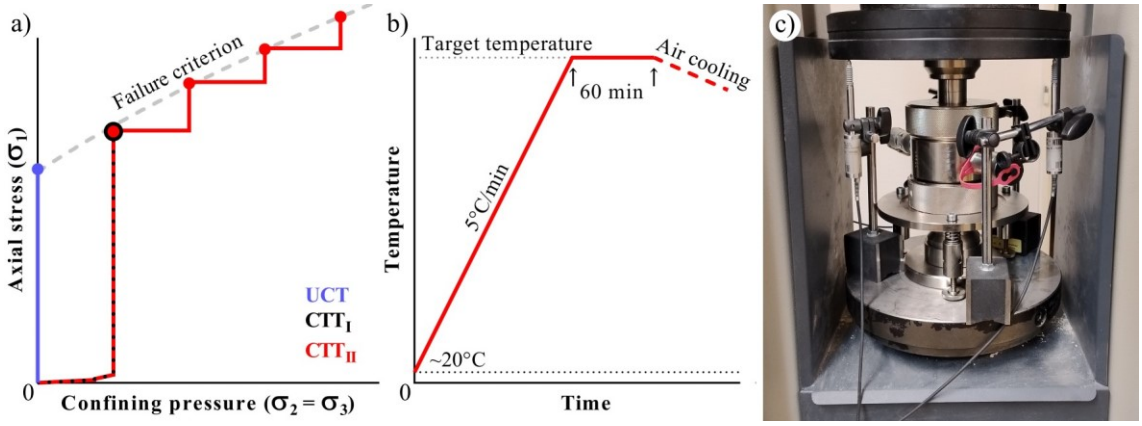

Fig. 1 a) Comparison of the UCT, CTT_I and CTT_{II} stress paths. b) Representative firing curve applied during specimen preparation. c) Hoek cell fitted with three LVDT sensors used for the realisation of the triaxial tests.

Mechanical testing was conducted using a CONTROLS testing setup equipped with a Hoek cell for triaxial test execution (in this case with 38.1 mm inner diameter, see Fig. 1c) and three LVDT sensors for displacement measurement. Both tests were controlled with a displacement rate, the UCTs with 2.5 µm/s and the CTT_{II}s with 1.0 µm/s (slower rate for lowering the risk of a premature specimen failure). The stress path used for the execution of the CTT_{II}s incorporates four different confinement steps (2, 4, 6 and 8 MPa; as in Fig. 1a) for the determination of four stress points close to the failure criterion (with the fifth being obtained from UCTs). The acquired stress points were subsequently plotted and fitted with an appropriate curve to determine the best-fit values of HB failure criterion parameters [5] – intact compressive strength (σ_{ci}) and intact rock constant (m_i). Disturbance and geological strength index were not considered under laboratory conditions (D = 0; GSI = 100). The stress-displacement diagram was used to assess the thermal damage based on the heat/unheated modulus ratio, following a method similar to [6].

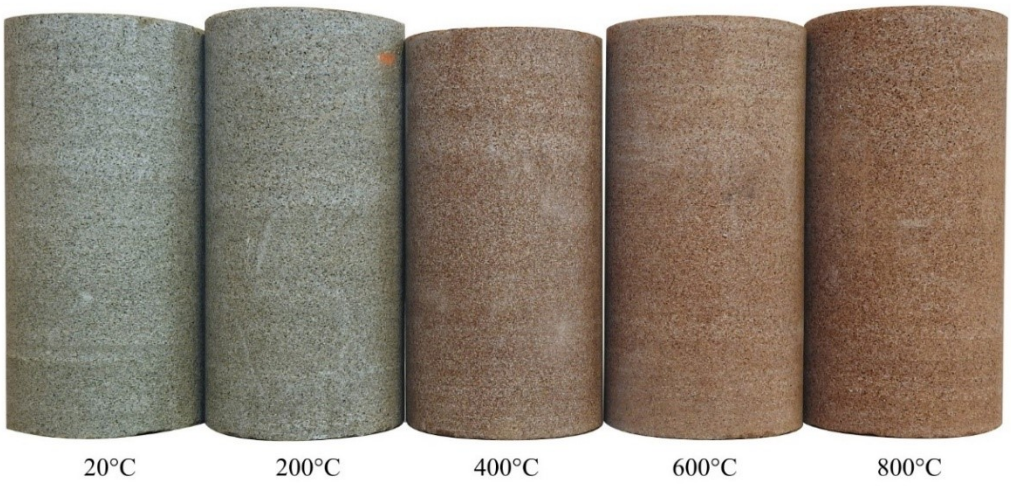

Fig. 2 The fired glauconitic sandstone specimens used for the CTT_{II}s (D = 38.1 mm, L/D ~ 2.0).

DOI 10.13164/juniorstav.2025.25032

3 RESULTS

The firing procedure resulted in a gradual visual alteration of the sampled glauconitic sandstone (Fig. 2). The sandstone in its natural state exhibits a predominantly greenish colour due to the presence of glauconite in its matrix (Fig. 3). As the target temperature increases, the matrix colour progressively shifts to a brick red, caused by the release of iron oxides [7] during the thermal alteration of the glauconite (Fig. 3). The framework grains, primarily composed of quartz, do not exhibit any significant visual alteration across the studied temperature range.

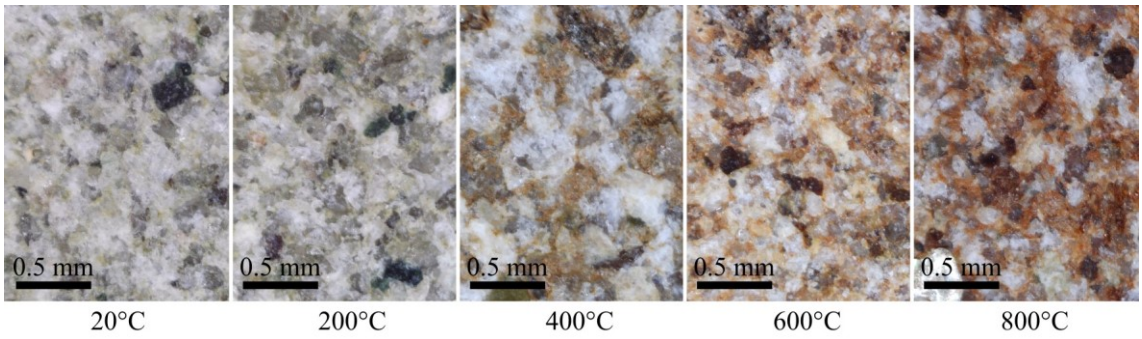

Fig. 3 The specimen bases displayed under a microscope.

The mechanical tests were generally successful (Fig. 4), though some minor complications arose. During the 200°C CTT_{II}, two loading steps (at 2 and 4 MPa confining pressure) were prematurely stopped and the obtained points were therefore not representing the real failure criterion. These points were easily identified and discarded due to their low σ_1 values and significant deviation from the other three points (both CTT_{II} and UCT). Similarly, during the 800°C CTT_{II}, a slight decrease in axial stress was observed, prompting an adjustment of the confining pressure to 3 MPa. Following this modification, the test proceeded as expected, and no data points were lost. Another issue occurred during the 600 and 800°C CTT_{II}s. A combination of high axial displacement necessary for the failure and progressive thermal disintegration of the matrix (leading to the detachment of many sand grains from the sheared fracture surfaces) resulted in major radial deformation of the specimen. This complicated the specimen removal and would pose a challenge for potential residual strength determination, which could otherwise be conducted after identifying the last peak point if desired.

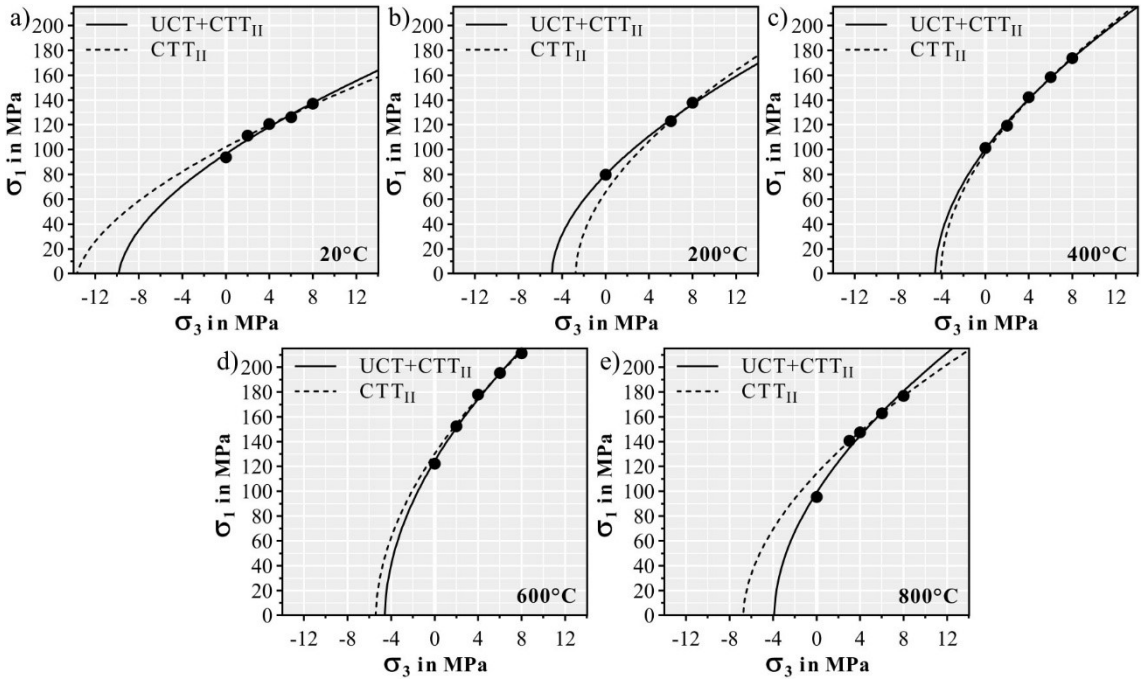

Fig. 4 Comparison of HB failure criteria derived from UCT + CTT_{II} results and CTT_{II} results only.

DOI 10.13164/juniorstav.2025.25032

The necessity of including an additional UCT alongside the CTT_{II} was evaluated by fitting both test results together and comparing them to the CTT_{II} results alone (Fig. 4). The difference was significant in some sets, indicating that the absence of the UCT could distort the obtained thermomechanical profile of the tested rock. This effect is even more pronounced in the trends of the individual HB parameters (Fig. 5b, d). The tensile strength of the rock, as predicted by the HB criterion, was also calculated and plotted for both cases (Fig. 5f). When the UCT was excluded, the tensile strength trend showed a steady increase after the initial drop. This deviated from the predictions, as it should decrease due to the glauconite matrix's gradual disintegration and the progressive development of microcracks as a result of the quartz α-β phase transition at 573°C [8]. The tensile strength trend aligns with the predictions with the UCT included, and thus confirms the progressive thermal damage to the rock.

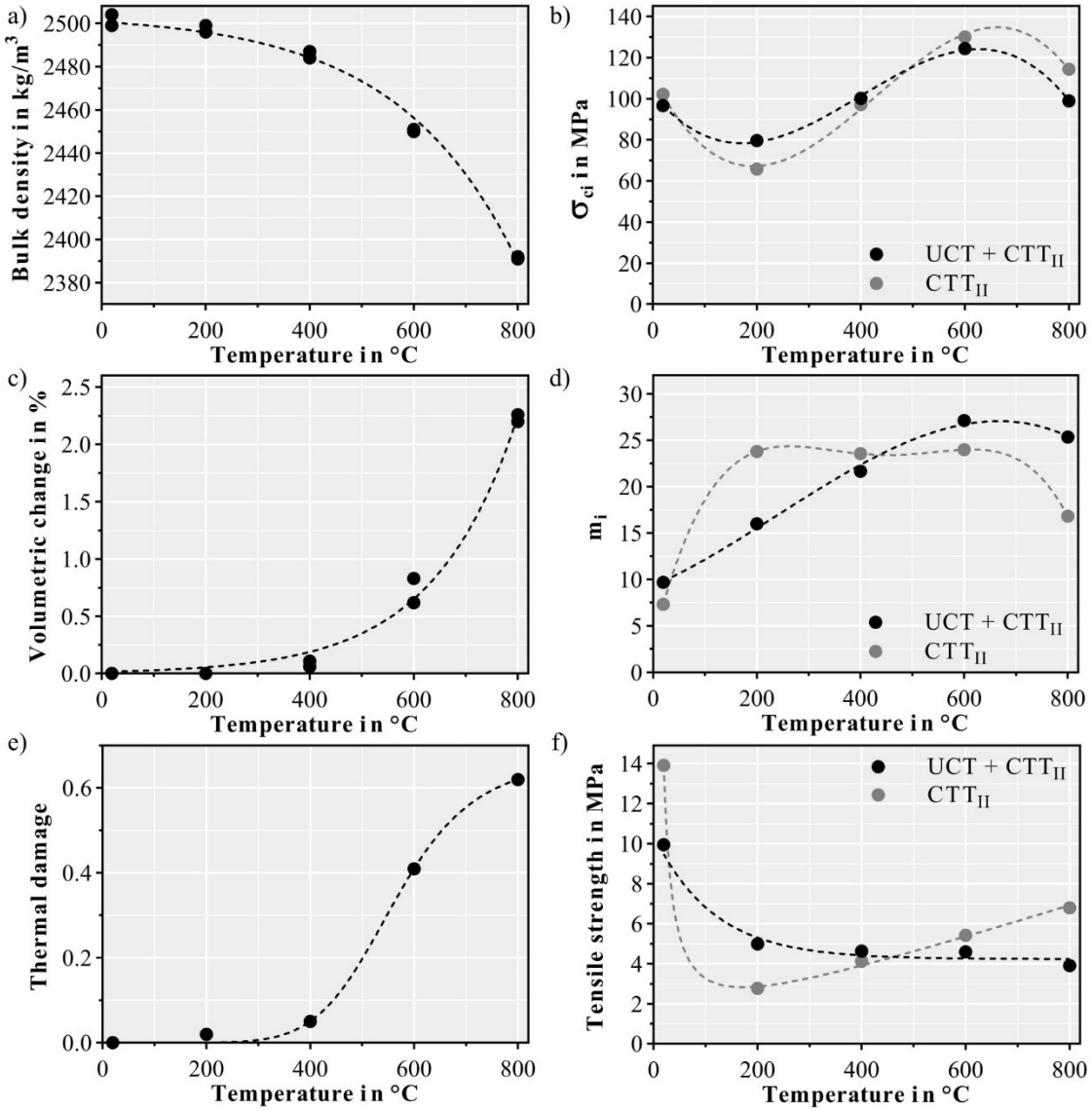

Fig. 5 Plots of the obtained sandstone properties dependence on the firing temperature with approximate fits.

The thermal damage was calculated according to [6] using the secant moduli [2] derived from stress-displacement diagrams (Fig. 5e). A stress range of 2–10 MPa was selected, as it falls safely within the nonlinear region of the diagram at the beginning of the loading sequence, before reaching the crack closure threshold [9]. This approach ensures that the thermal damage accounts for thermally induced crack development. It should be noted that the obtained moduli values are negatively affected by the measurement setup. Ideally, the moduli should be calculated from stress-strain diagrams obtained using strain gauges directly attached to the specimens [2]. However, the absolute values of the moduli are not critical for the damage calculation, only their ratio matters and it should remain unaffected using both measurement procedures. The continuous decrease of modulus value across the studied temperature range further supports the UCT + CTT_{II} tensile strength trend (Fig. 5f).

DOI 10.13164/juniorstav.2025.25032

A bulk density and volumetric change dependence on temperature was also obtained as a by-product of the performed thermomechanical study, These two characteristics are interconnected, as an increase in specimen volume leads to a decrease in bulk density. Consequently, both properties exhibit similar trends in opposite directions (Fig. 5a, c). The decrease in bulk density is further influenced by the gradual release of bonded water and mineral alteration. However, determining the exact cause would require further analyses.

4 DISCUSSION

Is the uniaxial compressive test necessary for a thermomechanical study?

Based on the presented findings, the incorporation of UCT in the set had a significant impact on the results and the obtained thermomechanical profile. Without the direct determination of the uniaxial compressive strength (or intact compressive strength according to the HB criterion terminology [5]), it must be extrapolated from the fit of CTT_{II} stress points. In this case, the first CTT_{II} point started at confining pressure $\sigma_3 = 2$ MPa, which is according to the experiment results (Fig. 5b) too far from the axis for a reasonably accurate σ_{ci} extrapolation. Additionally, the CTT_{II} performed on the 200°C specimen highlighted another reason for the UCT incorporation, as the CTT_{II} may in some cases yield an invalid stress point significantly deviating from the actual failure criterion. If multiple low-confining-pressure points were invalid, the extrapolation of σ_{ci} would be even less reliable. Therefore, we recommend performing the UCT, if a sufficient quantity of specimens is available.

Incorporating UCT is also beneficial for the thermal damage determination. As the cylindrical specimen shell is not obstructed by the Hoek cell during UCT, it allows for easier application of strain gauges for direct strain measurement. This enables a more accurate determination of deformation characteristics – moduli required for precise thermal damage calculation and potentially also Poisson's ratio.

Further improvement on the presented type II triaxial test procedure

The stress path of the CTT_{II} could potentially be improved to lessen the need for the execution of UCT and therefore to halve the material requirement. With a slight modification of the starting confining pressure to 0.5 MPa (or as low as the Hoek cell allows), the gap between the first stress point and the axis would be reduced, leading to more accurate σ_{ci} extrapolation. This possibility should be explored in subsequent research.

As demonstrated by the test results, CTT_{II} may present a slight risk of premature termination of the loading step, resulting in a stress point, which significantly deviates from the actual failure criterion. While the risk is not substantial (as it occurred in only two cases out of twenty loading steps performed), it could still be further minimised. Therefore, we recommend designing the CTT_{II} stress path with more than four loading steps, particularly when UCT is not performed. This approach should practically ensure the determination of a sufficient number of close-failure points for a reliable HB failure criterion description.

Is the generalised thermomechanical profile valid for marine psammitic sediments?

The thermomechanical parameters of the tested glauconitic sandstone appear to follow a trend similar to that of another marine psammitic sediment previously tested in our laboratory – greywacke [10]. To facilitate direct comparison, the HB failure criterion parameters of both rock types (σ_{ci}, m_i and predicted tensile strength) were therefore plotted as ratios of thermally altered to unaltered values (Fig. 6). Based on the available data, both marine sediments exhibit nearly identical behaviour, suggesting the potential for a generalised thermomechanical profile specific to marine psammitic sediments (after addition of more datasets).

Both the glauconitic sandstone and the greywacke share some similarities – both rock types are of marine origin with a dominant content of psammitic grains and with a high percentage of matrix based on clay minerals (glauconitic sandstone 5–15% [11]; greywacke by definition more than 15% [12]). However, there is a relatively clear difference in the mechanical properties of both sediments – the unaltered uniaxial compressive strength of the glauconitic sandstone is around 96 MPa, while the greywacke reached a strength of 146 MPa [10]. This 50 MPa difference can be attributed to the anchi-metamorphic nature of the greywacke as well as its higher bulk density.

DOI 10.13164/juniorstav.2025.25032

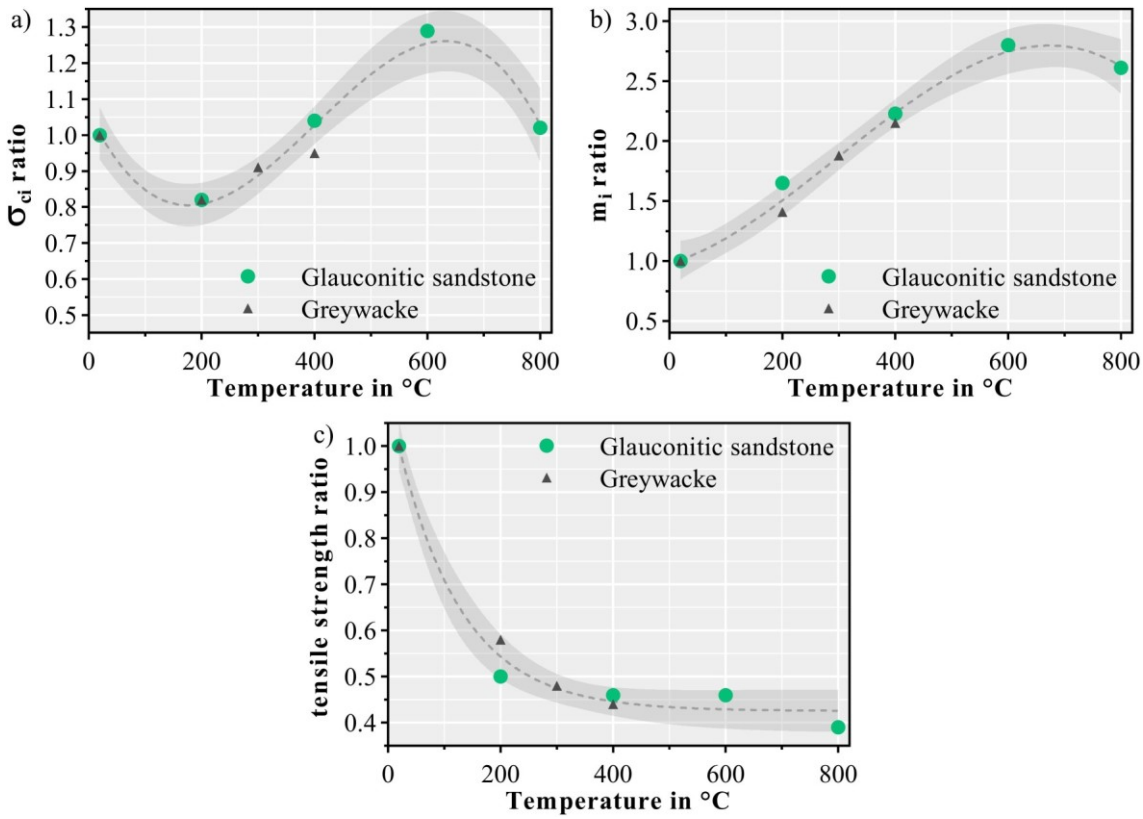

Fig. 6 Comparison of thermomechanical profiles of the glauconitic sandstone and previously tested greywacke (with approximate fits and 95% confidence intervals).

5 CONCLUSION

The objective of the presented experiment was successfully fulfilled – the general thermomechanical profile of the selected glauconitic sandstone was obtained with only ten specimens thanks to the implementation of the type II "multiple failure state" triaxial test. Several recommendations and findings emerged from the conducted tests:

- If possible, incorporate a uniaxial compressive test in every temperature step as extrapolating intact rock strength from type II triaxial test data only may lead to significant deviations, affecting the accuracy of the obtained thermomechanical profile.
- When an insufficient number of specimens is available for incorporation of the uniaxial compressive tests, the stress path of the type II triaxial test could be further modified to improve the extrapolation accuracy. By using a lower starting confining pressure value (e.g. 0.5 MPa), the first obtained stress point would be much closer to the axis, therefore lowering the distance of the extrapolated point from the actual measured data.
- The obtained thermomechanical profile of the glauconitic sandstone follows similar trends as previously tested greywacke. As both rock types are marine psammitic sediments, the presented data suggest the potential for a generalised thermomechanical profile applicable to all marine psammitic sediments.

Acknowledgements

This paper was written with the support of Brno University of Technology – Faculty of Civil Engineering, within grant No. FAST-S-24-8658.

References

[1] Haimson, B. and Bobet, A. Introduction to Suggested Methods for Failure Criteria. Rock Mechanics and Rock Engineering [online]. 2012, 45(6), pp. 973–974. ISSN 1434-453X. Availlable at: https://doi.org/10.1007/s00603-012-0274-6
[2] ASTM D7012-23. Standard Test Methods for Compressive Strength and Elastic Moduli of Intact Rock Core Specimens under Varying States of Stress and Temperatures. West Conshohocken: ASTM International, 2023. Availlable at: https://doi.org/10.1520/D7012-23
[3] Yang, S-Q., Tian W-L., Elsworth, D., Wang, J-G. and Fan, L-F. An Experimental Study of Effect of High Temperature on the Permeability Evolution and Failure Response of Granite Under Triaxial Compression. Rock Mechanics and Rock Engineering [online]. 2020, 53(10), pp. 4403–4427. ISSN 0723-2632, 1434-453X. Availlable at: https://doi.org/10.1007/s00603-019-01982-7
[4] Kovári, K., Tisa, A., Einstein, H. and Franklin, J. ISRM Suggested methods for determining the strength of rock materials in triaxial compression. International Journal of Rock Mechanics and Mining Sciences & Geomechanics Abstracts [online]. 1983, 20(6), pp. 285–290. ISSN 01489062. Availlable at: https://doi.org/10.1016/0148-9062(83)90598-3
[5] Hoek, E. and Brown, E. T. The Hoek–Brown failure criterion and GSI – 2018 edition. Journal of Rock Mechanics and Geotechnical Engineering [online]. 2019, 11(3), pp. 445–463. ISSN 16747755. Availlable at: https://doi.org/10.1016/j.jrmge.2018.08.001
[6] Xu, X-L., Karakus, M., Gao, F. and Zhang Z-Z. Thermal damage constitutive model for rock considering damage threshold and residual strength. Journal of Central South University [online]. 2018, 25(10), pp. 2523–2536. ISSN 2095-2899. Availlable at: https://doi.org/10.1007/s11771-018-3933-2
[7] Mashlan, M., Martinec, P., Kašlík, J., Kovářová, E. and Scucka, J. Mössbauer study of transformation of Fe cations during thermal treatment of glauconite in air. In: Mossbauer spectroscopy in materials science 2012: Proceedings of the International Conference MSMS-12, 11/06/2012–15/06/2012, Olomouc, Czech Republic [online]. Olomouc: AIP, 2012. Availlable at: https://doi.org/10.1063/1.4759486
[8] Ringdalen, E. Changes in Quartz During Heating and the Possible Effects on Si Production. JOM [online]. 2015, 67(2), pp. 484–492. ISSN 1047-4838. Availlable at: https://doi.org/10.1007/s11837-014-1149-y
[9] Wang, D., He, S. and Tannant, D. D. A Strain Based Method for Determining the Crack Closure and Initiation Stress in Compression Tests. KSCE Journal of Civil Engineering [online]. 2019, 23(4), pp. 1819–1828. ISSN 1226-7988, 1976-3808. Availlable at: https://doi.org/10.1007/s12205-019-0563-7
[10] Brabec, M., Krmíček, L., Sokolář, R., Štetiar, J. and Šimáček, R. Experimental Pilot Thermomechanical Study of Lower Carboniferous Greywacke: Temperature Effect on the Rock Mass Properties Investigated up to 1,200°C. Journal of Testing and Evaluation [online]. 2024, 52(5), 3149–3162. ISSN 0090-3973. Availlable at: https://doi.org/10.1520/JTE20240003
[11] Martinec, P., Vavro, M., Scucka, J. and Maslan, M. Properties and durability assessment of glauconitic sandstone: A case study on Zamel sandstone from the Bohemian Cretaceous Basin (Czech Republic). Engineering Geology [online]. 2010, 115(3–4), pp. 175–181. ISSN 00137952. Availlable at: https://doi.org/10.1016/j.enggeo.2009.08.005
[12] Okruchs, M. and Frimmel, H. E. Sediments and Sedimentary Rocks. In: Okruchs, M. and Frimmel, H. E., eds. Mineralogy: An Introduction to Minerals, Rocks, and Mineral Deposits [online]. Berlin, Heidelberg: Springer, 2020, pp. 417–452. ISBN 978-3-662-57316-7. Availlable at: https://doi.org/10.1007/978-3-662-57316-7_25